THE ASTROPHYSICAL JOURNAL, 408:507–513, 1993 May 10

AN OBSERVATION OF THE GALACTIC CENTER HARD X-RAY SOURCE, 1E 1740.7−2942, WITH THE CALTECH CODED-APERTURE TELESCOPE

WILLIAM A. HEINDL, WALTER R. COOK, JOHN M. GRUNSFELD,[1] DAVID M. PALMER,[2] THOMAS A. PRINCE, STEPHEN M. SCHINDLER, AND EDWARD C. STONE
Division of Physics, Mathematics, and Astronomy, California Institute of Technology, MS 220-47, Pasadena, CA 91125
Received 1992 May 5; accepted 1992 November 9

ABSTRACT

The Galactic center region hard X-ray source 1E 1740.7−2942 has been observed with the Caltech Gamma-Ray Imaging Payload (GRIP) from Alice Springs, Australia, on 1988 April 12 and on 1989 April 3 and 4. We report here results from the 1989 measurements based on 14 hr of observation of the Galactic center region. The observations showed 1E 1740.7−2942 to be in its normal state, having a spectrum between 35 and 200 keV characterized by a power law with an exponent of -2.2 ± 0.3 and flux at 100 keV of $(7.0 \pm 0.7) \times 10^{-5}$ cm^{-2} s^{-1} keV^{-1}. No flux was detected above 200 keV. A search for time variability in the spectrum of 1E 1740.7−2942 on one hour time scales showed no evidence for variability.

Subject headings: Galaxy: center — gamma rays: observations — X-rays: interstellar

1. INTRODUCTION

The source 1E 1740.7−2942 was discovered in soft X-rays (0.9–4 keV) with the *Einstein Observatory* in 1979 (Hertz & Grindlay 1984). In 1985, it was again observed in soft X-rays by Spartan 1 (Kawai et al. 1988) between 1 and 5 keV. The first hard X-ray identification, made using the coded mask telescope (SL2-XRT) on the Spacelab 2 mission (Skinner et al. 1987, 1989), showed 1E 1740.7−2942 to be the dominant source within the central few degrees of the Galaxy in the 20–30 keV band. Between 35 and 200 keV, 1E 1740.7−2942 was identified by the Caltech balloon-borne coded-aperture instrument, GRIP, in 1988 (Cook et al. 1989, 1990, 1991b). In these observations, 1E 1740.7−2942 was found to be the brightest Galactic center hard X-ray source, having a strong power-law spectrum extending up to 200 keV. GRIP again observed 1E 1740.7−2942 on 1989 April 3–4 (Grunsfeld et al. 1991). The results of this observation are presented here.

The Galactic center region has also been observed at hard X-ray energies by the balloon-borne telescope EXITE (~1 month after the 1989 GRIP observation) (Covault, Manandhar, & Grindlay 1990), the HEXE and TTM instruments on *MIR* (Skinner et al. 1991), and the ART-P and SIGMA instruments aboard the *GRANAT* spacecraft (Sunyaev et al. 1990, 1991; Paul et al. 1990; Bouchet et al. 1991; Schmitz-Fraysse et al. 1992). With the exception of a subset of the SIGMA observations (see below), all of these instruments found the energy spectrum of 1E 1740.7−2942 to be similar to the GRIP 1988 spectrum, defining a "normal" state of the source. The SIGMA observations showed that in addition to this normal state, 1E 1740.7−2942 has both a "hard" and a "low" emission state (Sunyaev et al. 1991).

The "hard" spectrum (Bouchet et al. 1991) is characterized by the normal power-law spectrum below 200 keV, but exhibits a rising continuum spectrum above 200 keV, peaking near 500 keV, and cutting off above 700 keV. This state was seen by SIGMA only during an observation on 1990 October 13–14. A probable source of this feature is e^+e^- annihilations in a hot pair plasma (Bouchet et al. 1991). Observations by SIGMA on 1990 October 11 and 15 found 1E 1740.7−2942 in its normal emission state, indicating that the hard state lasted between 18 and 70 hr. This variability on a time scale of a few days or less limits the emission region to a size of a few times 10^{15} cm. Although no narrow line annihilation radiation has been reported for this period, the fact that the feature is centered near the positron annihilation energy makes 1E 1740.7−2942 a likely candidate for the compact source of positron annihilation radiation near the Galactic center required by the observed time variable 511 keV flux (Riegler et al. 1981, 1985; Lingenfelter & Ramaty 1989; Gehrels 1991).

The "low" emission state of 1E 1740.7−2942 (Sunyaev et al. 1991) is characterized by emission in the power-law region (30–200 keV) ~20% or less of that observed in the normal state, with no detectable emission above 200 keV. Between the 1990 October and 1991 February SIGMA Galactic center observations, 1E 1740.7−2942 entered this state and apparently remained at a low flux level until at least 1991 April (Sunyaev et al. 1991). It has also been reported (Bazzano et al. 1992) that the narrow (1°.9 FWHM) field of view (FOV) balloon-borne instrument, POKER, detected 1E 1740.7−2942 in this low state just 6 weeks after the 1989 GRIP observations and 2 weeks after the EXITE observations.

Observations made with the Very Large Array (VLA) (Prince, Kulkarni, & Skinner 1991b) have revealed a weak radio source (source "A") within the 12″ radius X-ray error circle for 1E 1740.7−2942, as determined by TTM (Skinner et al. 1991). Furthermore, a preliminary 5″ radius error circle for 1E 1740.7−2942 based on a *ROSAT* high-resolution imager (HRI) observation at 0.1–2 keV includes source "A" (Prince et al. 1991a). Recent VLA observations (Mirabel et al. 1992) have found that source "A" lies at the center of an aligned double radio jet. Millimeter wavelength observations have recently shown a molecular cloud in line of sight coincidence with 1E 1740.7−2942, suggesting a possible association (Bally & Leventhal 1991; Mirabel et al. 1991) with the resulting possibility that Bondi-Hoyle accretion onto a black hole moving through interstellar gas could be the source of the hard X-ray luminosity.

[1] Current address: NASA Johnson Space Flight Center, Code CB, Houston, TX 77058.
[2] Current Address: NASA Goddard Space Flight Center, Code 661, Greenbelt, MD 20771.

In this paper, we discuss our 1989 observations of 1E 1740.7−2942 in the energy range 30 keV to 7.5 MeV. We present a measurement of the hard X-ray spectrum as well as a search for time variability of the spectrum in the power-law region, 35–200 keV, and the "bump" region, 300–600 keV. Preliminary results of this analysis were presented in Grunsfeld et al. (1991).

2. OBSERVATIONS

The observations reported here were performed with the Caltech Gamma-Ray Imaging Payload (GRIP), a balloon-borne coded-aperture telescope sensitive to photons in the energy range 30 keV to 10 MeV (Althouse et al. 1985). The detector system consists of a rotating hexagonal uniformly redundant array (HURA) which modulates the sky flux incident on an actively shielded, position-sensitive NaI(Tl) scintillation detector. A lead hexcell collimator (added since Althouse et al. [1985]) reduces the contribution of the diffuse aperture flux to the background. For these observations, GRIP was configured for 1°1 angular resolution over a 14° FOV. An image-intensified CCD star camera and a second CCD camera for viewing bright stars and planets are employed to obtain precise aspect solutions for observations made during nighttime hours. During daylight conditions, telescope orientation is determined from a set of inclinometers and magnetometers. An on-board altimeter and the OMEGA radio navigation system give the physical location of the gondola.

GRIP observed the Galactic center region for 16.3 hr during a 42 hr flight beginning 1989 April 3 from Alice Springs, NT, Australia. Because 1E 1740.7−2942 may have been obscured by the gondola suspension during the Galactic center transit, 2.3 hr of data have not been used in this analysis. Thus, the results from a total observation time on the Galactic center region of 14.0 hr are presented here. Approximately half of the observation occurred during the night, when precise pointing aspect is determined from the star camera system. Because of the failure of a trigger circuit which provides event tags for the decay photons from an on-board calibration source, data in the energy range 46–71 keV were contaminated with 60 keV ^{241}Am line photons and have not been used in the analysis.

3. ANALYSIS

3.1. *Aspect Determination*

The two CCD star cameras described above have FOVs which are offset from the γ-ray telescope axis. This allows them to provide useful data even when the γ-ray telescope points through the balloon. Analysis of images from the two cameras determines an axis of the CCD camera platform which is nearly parallel to the imaging axis of the γ-ray telescope. The offset between these axes is calibrated through in-flight observations of the Crab Nebula and Pulsar and verified through observations of Cygnus X-1. For the Galactic center observations, offsets determined from the camera system were used in postflight analysis to correct images for errors in the real-time pointing. The primary source of error in aspect determination using the camera system is the statistical uncertainty in the location of the Crab in the γ-ray image used to calibrate the camera system offset. The resulting one dimensional rms uncertainty in image positions is ∼4′. Any detected source will have an additional position uncertainty due to the location statistics of its image peak.

During daylight hours, when no star camera data were available, the γ-ray data were divided into time periods using two approaches. For analysis of the overall spectrum, the periods were chosen such that in each period an image source peak was detected at a significance of at least 5 σ in the energy range 35–200 keV. The source flux was then determined from the image value at the peak location (see § 3.2). Calculating the flux based on the image value at the peak, rather than at the nominal source location, introduces a systematic flux overestimate in these periods of less than 5%, but is insensitive to residual pointing errors which may be present in the daytime data. These periods varied in length between 0.5 and 1.7 hr. For the time variability analyses, where the choice of time periods by measured source peak significance may bias the overall measurement, locations were determined from images incorporating ∼2 hr of data. These data were then divided into 0.9–1.3 hr periods, and fluxes were calculated at the previously determined source locations.

3.2. *Flux Determination*

A detailed treatment of the method by which source fluxes in individual energy bins are determined is given in the Appendix. A brief summary of the method used is given here.

Source fluxes are determined using a modification of the trial spectrum method described by Fenimore, Klebesadel, & Laros (1983). In this technique, a model spectral form is integrated with the instrument response function in order to derive a predicted count spectrum. In analysis of data from a coded-aperture instrument, the predicted and measured count spectra are replaced by predicted and measured "image values." The set of image values is analogous to the count spectrum in a nonimaging instrument, but also includes effects due to the imaging properties of the coded-aperture instrument. A goodness of fit parameter (e.g., χ^2) is employed to determine which of several trial model spectra best fits the data. The best-fit model spectrum is then used to derive flux values in individual energy bins.

In the analyses described here, two input spectral forms were used. The first was a standard power-law form. The second, which was used to search for emission from 1E 1740.7−2942 between 300 and 600 keV, was the Gaussian line profile (mean = 480 keV, FWHM = 240 keV) given by Bouchet et al. (1991).

4. RESULTS

4.1. *Imaging*

Figure 1 shows an image of the Galactic center region for the energy range 35–200 keV obtained using the 7.4 hr of data for which a complete aspect solution was available from the star camera system. A single bright hard X-ray source is visible, located 8′ from the expected location of 1E 1740.7−2942. Figure 2 is an expanded view of the source region, showing the 90% confidence error circle for the location of the source. The error circle is ∼24′ in diameter and includes uncertainties arising from the aspect determination (cf. § 3.1) and source peak location statistics. The error circle excludes all other known hard X-ray sources.

It should be noted that in Figure 1, a peak of greater than 2 σ significance appears at the expected location of GRS 1758−258. During these observations GRS 1758−258 was well off the collimator axis (14° FWHM) and was therefore observed with reduced sensitivity. Although the peak in Figure

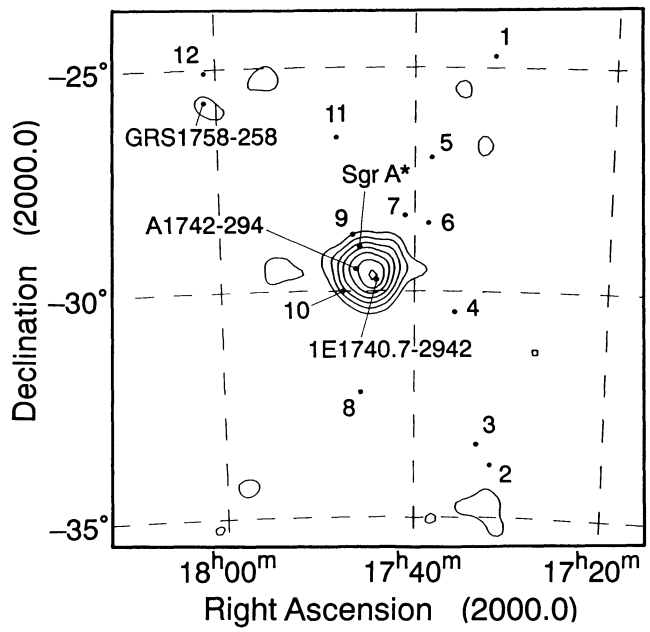

FIG. 1.—GRIP image of the Galactic center region from 35 to 200 keV on 1989 April 3, 4. The contours indicate the number of excess counts in a given direction, calibrated in units of the statistical significance of the excess, with contours beginning at the 2 σ level and spaced by 1 σ. Known hard X-ray sources (Levine et al. 1984; Skinner et al. 1987; Paul et al. 1990; Cook et al. 1991a) are (1) GX 1+4, (2) GX 354+0, (3) MXB 1730−335 ("Rapid Burster"), (4) SLX 1732−304, (5) SLX 1735−269, (6) GX 359+2, (7) SLX 1737−282, (8) A1743−322, (9) 1E 1743.1−2843, (10) SLX 1744−299, (11) GX 3+1, (12) GX 5−1.

1 is too small to provide a firm detection, a measurement of the flux from the location of GRS 1758−258 incorporating all 14.0 hr of Galactic center data yields a 3.6 σ result in the energy range 35–200 keV. It therefore seems likely that this peak is due to GRS 1758−258. Assuming an E^{-2} power-law spectrum (Sunyaev et al. 1990), the 100 keV source flux for GRS 1758−258 would be $(2.6 \pm 0.7) \times 10^{-5}$ cm^{-2} s^{-1} keV^{-1}. This value is somewhat lower than the 100 keV flux of $(4.8 \pm 0.3) \times 10^{-5}$ cm^{-2} s^{-1} keV^{-1} derived from SIGMA observations of 1990 March–April and September–October (Sunyaev et al. 1990); however, the difference is not surprising given the observed variability of GRS 1758−258 (Cordier et al. 1991).

Also in the FOV during these observations was the burst source GX 354+0. In 1988, GRIP detected GX 354+0 near its maximum nonburst brightness (Cook et al. 1991a, b), having a flux of ~100 mCrab between 35 and 122 keV. It has recently been seen by SIGMA at a flux level of 75 mCrab (Gilfanov et al. 1992). GX 354+0 was not detected in the 1989 GRIP observations. Employing a flat input spectrum (a power law with an exponent of zero) yields a 95% confidence upper limit to the flux from GX 354+0 of 1.8×10^{-5} cm^{-2} s^{-1} keV^{-1} (~10 mCrab) in an energy band from 35 to 122 keV.

4.2. *Spectrum*

The photon number spectrum for 1E 1740.7−2942, based on all 14.0 hr of data (both daytime and nighttime periods), is shown in Figure 3. Above 200 keV, no significant flux was detected from 1E 1740.7−2942, and upper limits at the 95% confidence level for energy bands above 200 keV are given in Figure 3. A flux measurement made in a 90 keV wide energy band centered near 511 keV, with a narrow positron annihilation line input spectrum, gives a 95% confidence upper limit to the 2γ positron annihilation radiation flux from 1E 1740.7−2942 of 3.7×10^{-4} cm^{-2} s^{-1}.

Between 35 and 200 keV, the data are well fitted (cf. eq. [A2]) by a single power law $[dJ/dE = K(E/100 \text{ keV})^{-\gamma}]$, with a spectral slope of $\gamma = 2.2 \pm 0.3$ and flux normalization of $K = (7.0 \pm 0.7) \times 10^{-5}$ cm^{-2} s^{-1} keV^{-1}. Parameter errors are defined by an increase of 2.3 in χ^2, appropriate for a two-parameter fit and 68% confidence (Lampton, Margon, & Bowyer 1976; Avni 1976). Figure 4 shows confidence regions for this fit at the $\chi^2_{\min} + 1$ and $\chi^2_{\min} + 2.3$ levels.

Figure 5 shows the time history of the 35–200 keV luminosity, calculated from the integral of the $E^{-2.2}$ power-law fit and assuming a source distance of 8.5 kpc. Fitting the measurements to a single luminosity yields a value of $(1.7 \pm 0.1) \times 10^{37}$ ergs s^{-1}, with a reduced χ^2 of 1.61 with 11 degrees of freedom (d.o.f.). The probability of exceeding this χ^2 is 9%, giving no strong evidence for variability on these time scales.

The sensitivity of GRIP makes it possible to search on hour time scales for the presence of a feature such as the 300–600 keV excess observed by SIGMA. The 95% confidence level upper limits to the flux in the 300–600 keV region are shown in Figure 6. Variations in the upper limits are due to the time-variable atmospheric depth of the observations and statistical fluctuations in the images. Also shown in Figure 6 is the combined upper limit from the entire observation and the flux level from the SIGMA 1990 October measurement. It is apparent that on hour time scales during the GRIP observation, the 300–600 keV excess was not present at the level seen by SIGMA.

5. DISCUSSION

The GRIP 1989 April spectrum for 1E 1740.7−2942 is very similar to those measured by GRIP in 1988 April (Cook et al. 1989, 1990, 1991b), EXITE in 1989 May (Covault et al. 1990), SIGMA in 1990 March, April, and September (Sunyaev et al. 1990, 1991; Paul et al. 1990; Bouchet et al. 1991; Schmitz-Fraysse et al. 1992), and by HEXE in 1989 March (Skinner et al. 1991) (see Fig. 7, discussed below). The consistency of these measured spectra in the period 1988–1990 serves to define the "normal" emission state and suggests that this state was predominant over a period of years. No variability was reported for 1E 1740.7−2942 prior to the discovery of the hard state by SIGMA. Recently, however, Bazzano et al. (1992) reported that on 1989 May 9, just 6 weeks after the GRIP observation, 1E 1740.7−2942 was in the low state. The time scale of this variability implies a size of less than 4×10^{17} cm for the hard X-ray emission region. A stronger limit of less than 10^{17} cm is set using the EXITE observation which occurred 4 weeks after the GRIP observation. This can be compared with the upper limit from the SIGMA observations of a few times 10^{15} cm for the region responsible for the excess hard state emission. Although these limits differ by almost two orders of magnitude, they cannot rule out a single region for both the normal and hard state emissions.

The spectra from imaging and narrow FOV (<2°) hard X-ray observations of 1E 1740.7−2942 prior to 1990 October are shown together in Figure 7. The close agreement between the normal state measurements, made with several different instruments, is notable. The normal state spectrum between 35 and 200 keV is similar to the γ_2 and γ_3 states of Cygnus X-1 (Ling et al. 1987; Cook et al. 1991b) both in spectral shape and

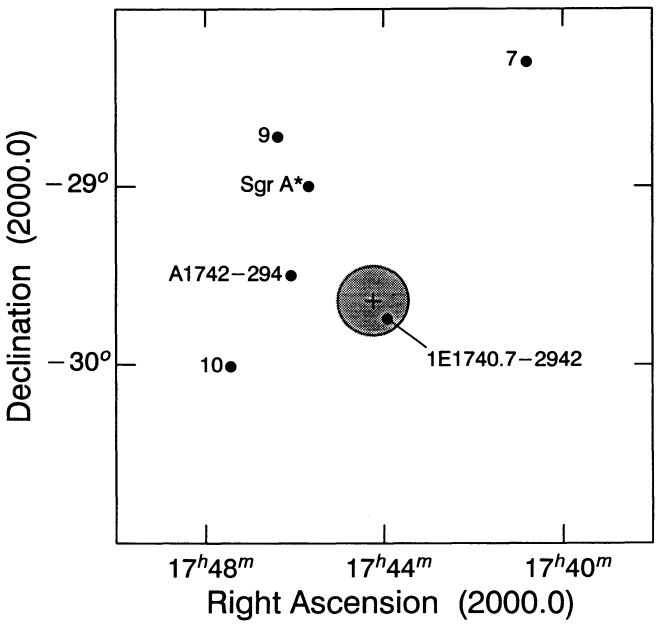

FIG. 2.—Expanded view of the source region showing the 90% confidence error circle for the location of the γ-ray source. Only 1E 1740.7−2942 appears within the error circle. Known hard X-ray sources are numbered as in Fig. 1.

total luminosity. Because of these similarities, it is natural to speculate that similar processes are at work in both systems. Cygnus X-1 is believed to be a stellar mass black hole accreting from its blue supergiant companion. Its spectrum has been well

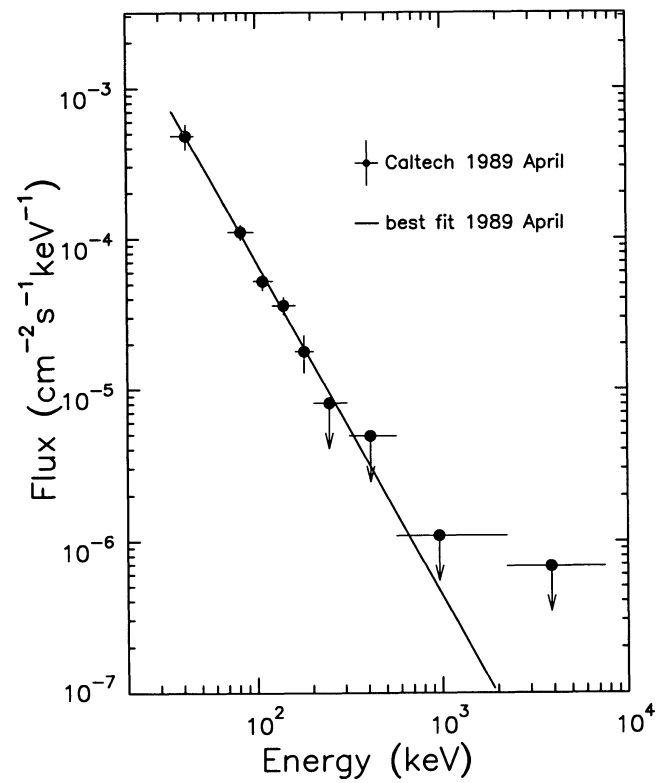

FIG. 3.—Photon number spectrum of 1E 1740.7−2942. Upper limits are at the 95% confidence level. Also shown is the best fit power-law spectrum $[dJ/dE = K(E/100\ \text{keV})^{-\gamma}]$: $K = (7.0 \pm 0.7) \times 10^{-5}$ cm^{-2} s^{-1} keV^{-1}, $\gamma = 2.2 \pm 0.3$.

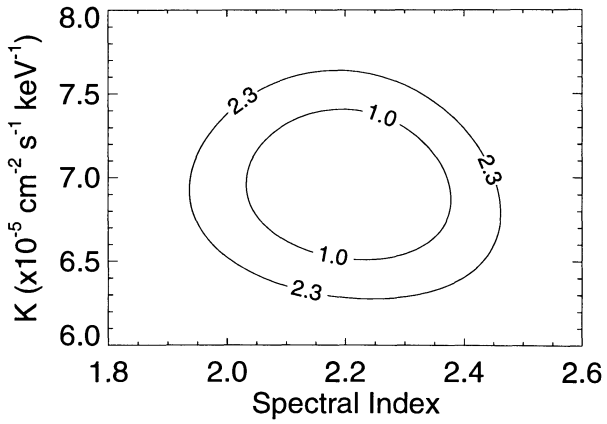

FIG. 4.—χ^2 contours for the power-law fit in Fig. 3. Contours are at $\chi^2_{min} + 1$ and $\chi^2_{min} + 2.3$, where χ^2_{min} is the value for the best-fit parameters. These levels give 68% confidence regions for one and two parameter fits, respectively. The reduced χ^2 of the two parameter fit is 1.0 for 58 d.o.f.

fitted using a Comptonized model (Liang & Dermer 1988; Sunyaev & Titarchuk 1980). Fitting a Sunyaev & Titarchuk (1980) Comptonized spectrum to the derived fluxes in Figure 3 yields an electron temperature of $kT \approx 50$ keV and an optical depth of 2. Because of the energy range of the GRIP flux measurements, these values are not well constrained, although

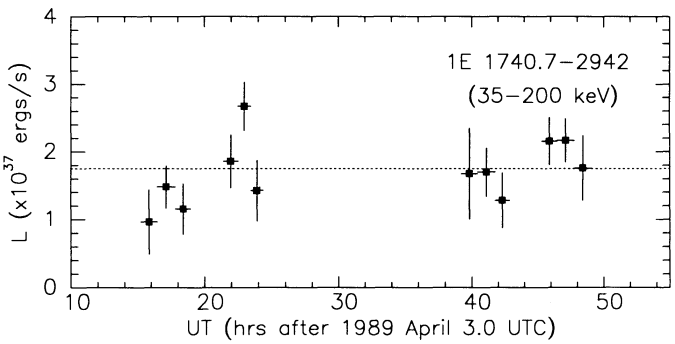

FIG. 5

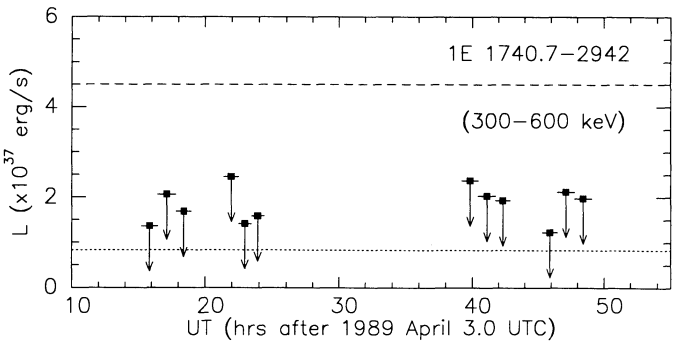

FIG. 6

FIG. 5.—Time history of the 35–200 keV luminosity of 1E 1740.7−2942, assuming a source distance of 8.5 kpc. The best-fit constant flux level is indicated by the dashed line and has a reduced χ^2 of 1.61 for 11 d.o.f.

FIG. 6.—95% confidence upper limits to the 300–600 keV luminosity of 1E 1740.7−2942 as a function of time, assuming a source distance of 8.5 kpc. The dashed line is the flux level seen by SIGMA on 1991 October 13–14 (Sunyaev et al. 1991). Integrating the SIGMA "bump" spectrum from Bouchet et al. (1991) gives a somewhat higher value for the 300–600 keV luminosity. The dotted line shows the overall limit for the entire GRIP observation.

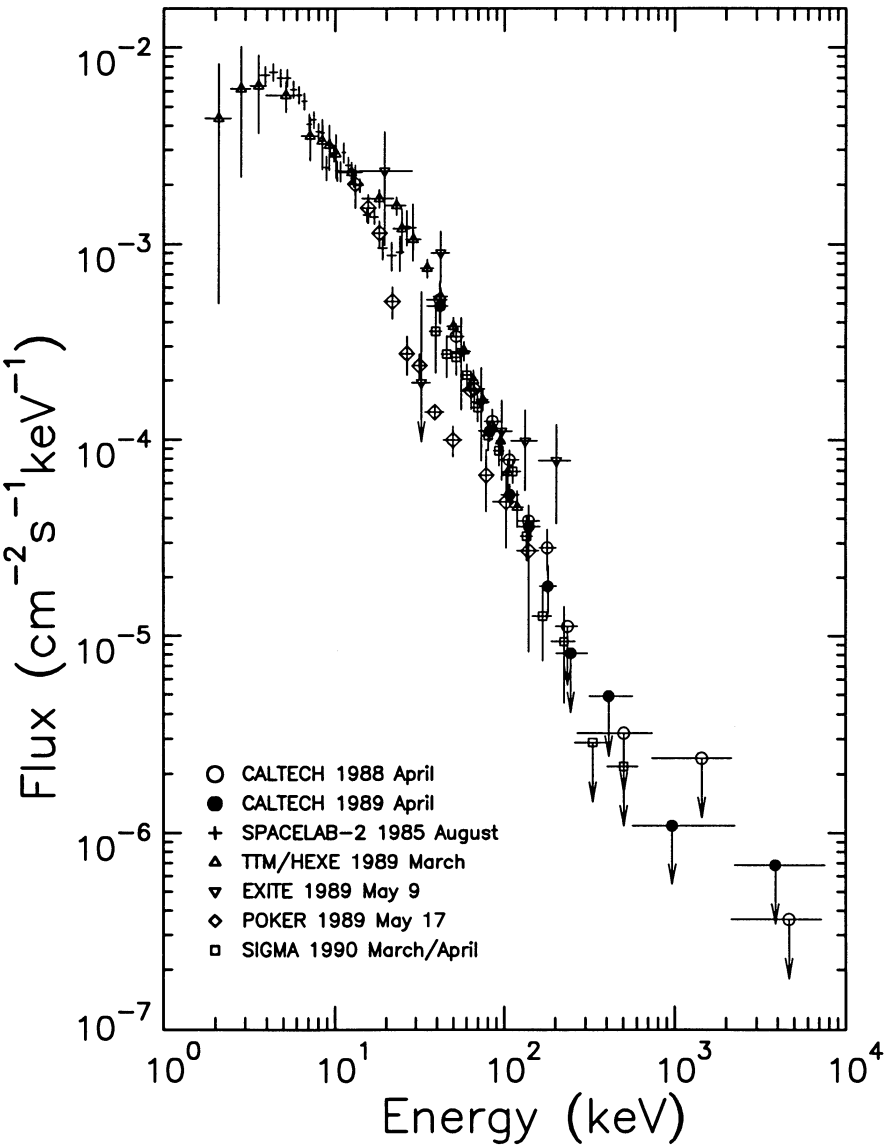

FIG. 7.—Comparison of 1E 1740.7−2942 imaging and narrow FOV spectra. Shown are spectra from all hard X-ray imaging and $<2°$ FOV observations made prior to 1990 October (Cook et al. 1991a; Skinner et al. 1989, 1991; Covault et al. 1990; Bazzano et al. 1992; Bouchet et al. 1991). With the exception of Bazzano et al. (1992), all these observations found 1E 1740.7−2942 to be in its "normal" state.

they are consistent with those measured by SIGMA (Sunyaev et al. 1991) and HEXE (Skinner et al. 1991).

Although the normal state of 1E 1740.7−2942 appears to have been stable on long time scales, it is interesting to ask if this apparent long-term stability of the power-law continuum might overlie variability on shorter time scales, as seen in Cygnus X-1. While the results shown in Figure 5 may appear to give some indication of variability, they do not strongly contradict a constant flux. We conclude that the power-law spectrum was relatively stable on hour time scales during the GRIP observation. This is in agreement with the HEXE result (Skinner et al. 1991), which reported no variability in 1E 1740.7−2942 on time scales from minutes to months.

An intriguing observational question concerning the Galactic center region is the nature of the time variable positron annihilation radiation seen there. The first evidence of variability came from observations made with the *HEAO 3* satellite, which showed a significant decrease in 511 keV emission from the Galactic center region between the fall of 1979 and spring of 1980 (Riegler et al. 1981, 1985). Between 1988 May and October, the GRIS balloon-borne germanium spectrometer detected an increase in 511 keV line radiation, finding fluxes inconsistent with a constant value at the 95% confidence level (Gehrels et al. 1991). A measurement with another balloon-borne germanium spectrometer, the UCSD/France instrument HEXAGONE, in 1989 May (Chapuis et al. 1991), only 7 weeks after the GRIP flight, showed the line flux to again have decreased to a level consistent with known diffuse Galactic plane emission (Gehrels 1991). The SIGMA "bump" emission, which is likely the result of e^+e^- annihilations in a hot pair plasma (Bouchet et al. 1991), seems to be another signature of the action of positrons, this time from a definite source: 1E 1740.7−2942. In fact, such direct evidence of the presence of positrons associated with 1E 1740.7−2942 makes it a very

strong candidate for the variable 511 keV source. However, the lack of narrow line emission prevents a positive identification. Thus, the identification of the 511 keV source awaits an imaging experiment to detect the direct annihilation photons.

The GRIP 95% confidence upper limit of 3.7×10^{-4} cm^{-2} s^{-1} for 511 keV line flux from 1E 1740.7−2942 is significantly lower than the limit of 6.8×10^{-4} cm^{-2} s^{-1} obtained by GRIP for 1E 1740.7−2942 in 1988 (Cook et al. 1991a). Gehrels (1991) derived a compact source strength of $(3.9 \pm 2.7) \times 10^{-4}$ cm^{-2} s^{-1} from the HEXAGONE measurement by subtracting a contribution based on a model of the diffuse Galactic plane 511 keV emission having a flat distribution and a strength of 1.2×10^{-3} cm^{-2} s^{-1} rad^{-1}. This is in agreement with the GRIP upper limit, and both measurements are below the level of $(7.8 \pm 1.6) \times 10^{-4}$ cm^{-2} s^{-1} derived for the GRIS 1988 October measurement (Gehrels 1991). Therefore, if 1E 1740.7−2942 were the compact source of annihilation photons seen by GRIS, it subsequently entered a low or off state.

We acknowledge the important contributions to the development of the GRIP telescope made by W. Althouse, D. Burke, A. Cummings, M. Finger, C. Starr, J. Weger, and the personnel of the Central Engineering Services at Caltech. We thank the personnel of the National Scientific Balloon Facility and the NASA Wallops Flight Facility for their excellent balloon launch support. This work was supported in part by NASA grant NAGW-1919. W. Heindl is supported under the NASA GSRP, NGT-50804.

APPENDIX

SOURCE FLUX DETERMINATION

In X-ray and gamma-ray astronomy it is desirable to give the detector count spectrum as well as the deconvolved source flux spectrum. The former gives a model-independent representation, but can have a strong instrumental signature. The latter gives a model dependent estimate of the actual source spectrum, removing to a large extent the instrumental signature by taking into account the instrument response matrix. In the case of GRIP, it is not possible to give a simple instrument count spectrum, because parameters such as line of sight atmospheric depth and collimator transmission for a given source direction vary over the duration of an observation. Therefore we give source flux values for individual energy bins which are as model independent as possible.

In an instrument with perfect energy resolution (i.e., a source photon of energy E is always detected with energy E, or equivalently, the instrument response matrix is diagonal), the determination of the photon flux in a given energy bin is independent of the true spectral shape of the source. Because only photons with energies in a particular bin contribute to that bin, the source flux may be directly determined from the count spectrum and the (diagonal) detector response matrix.

However, for an instrument with finite energy resolution, the nature of the source spectrum affects the determination of fluxes through the off-diagonal terms in the response matrix. For example, for a source with a steep spectrum, photons with energies below a given energy bin may contribute significantly to the counting rate in that bin. At the same time, photons with energies within that bin will be lost to nearby bins. Therefore, in order to account for these effects, the determination of fluxes in individual energy bins must make some assumption about the true nature of the source spectrum. Because our aim is to produce a model-independent flux spectrum, it is desirable that these assumptions have a minimal effect on the derived fluxes. Our approach is to employ the best-fit spectral shape, as determined from the full set of energy bins, to the derivation of fluxes in individual energy bins. We then verify that varying the assumed spectral shape has only a small effect on the resultant flux values. When no positive flux is detected in a given energy bin, a flat spectrum (i.e., a power law with a spectral index of 0) is assumed for the purpose of setting upper limits.

As mentioned in § 3.2, the source flux values are estimated using a forward convolution method. The data are first divided into time periods over which variations in parameters such as atmospheric depth and source attenuation due to the collimator are small. For each period, an image is produced for each energy bin of interest. These images, derived from disjoint data sets, are statistically independent.

The image values at the source location in the individual images are designated $i_{\alpha n}$, where α denotes the time period and n the energy bin. A spectral class, $dJ/dE(\psi, E)$, with N adjustable parameters, $\psi = (\psi_0, \psi_1, \ldots)$, is then chosen as a set of model spectra. As applied here, one of the parameters is an overall normalization, while the others (e.g., the spectral index in a power law) determine the spectral shape.

The parameters, ψ, are varied over a physically reasonable range, with each set of values corresponding to a separate model spectrum. To determine χ^2 for a given model, the model spectrum is integrated with the instrument response function, $R_{\alpha n}(E)$, appropriate for each time period and energy bin. The response function includes the time-dependent effects of varying atmospheric depth and collimator attenuation, as well as energy-dependent effects such as attenuation in passive instrument material, the energy resolution and position resolution of the detector, and the overall imaging properties of the instrument. This integration produces a set of predicted image values, $\hat{i}_{\alpha n}(\psi)$, corresponding to the measured image values $i_{\alpha n}$.

$$\hat{i}_{\alpha n}(\psi) = \int_0^\infty \frac{dJ}{dE}(\psi, E) R_{\alpha n}(E) dE \; ; \tag{A1}$$

χ^2 is then given by

$$\chi^2 = \sum_\alpha \sum_n \left\{ \frac{[i_{\alpha n} - \hat{i}_{\alpha n}(\psi)]^2}{\sigma_{\alpha n}^2} \right\} \tag{A2}$$

where $\sigma_{\alpha n}$ is the standard deviation in the measured image value and depends only on the energy bin, n, and the number of events contributing to the image. Because almost all GRIP observations are background dominated with a large number of events contributing to each image, $\sigma_{\alpha n}$ is model independent, and may be determined from the measured number of counts contributing to the image. The model parameters which minimize χ^2 define the best-fit spectral shape and are denoted ψ^*, with ψ_0^* as the overall normalization.

Once a spectral shape has been determined, the source fluxes in individual energy bins may be determined. This is done by integrating the best fit spectral shape, employing unit normalization ($\psi_0^* = 1$), with the instrument response function to get a second set of predicted image values, $\hat{i}_{\alpha n}(\psi^*; \psi_0^* = 1)$. The flux normalization in a given energy bin for a specific time period is then

$$\kappa_{\alpha n} = \frac{i_{\alpha n}}{\hat{i}_{\alpha n}(\psi^*; \psi_0^* = 1)}, \tag{A3}$$

with the statistical uncertainty in $\kappa_{\alpha n}$ given by

$$\sigma_{\kappa_{\alpha n}} = \frac{\sigma_{\alpha n}}{\hat{i}_{\alpha n}(\psi^*; \psi_0^* = 1)}. \tag{A4}$$

A weighted average of the $\kappa_{\alpha n}$ over the time periods, α, then gives the flux normalization for the energy bin n:

$$\bar{\kappa}_n = \left(\frac{\sum_\alpha \kappa_{\alpha n}/\sigma^2_{\kappa_{\alpha n}}}{\sum_\alpha 1/\sigma^2_{\kappa_{\alpha n}}} \right). \tag{A5}$$

The flux, $F_n(E_n)$, is then given by

$$F_n = \bar{\kappa}_n \times \frac{dJ}{dE}(\psi^*; \quad \psi_0^* = 1; \quad E = \bar{E}_n) \tag{A6}$$

where $\bar{E}_n$ is the mean energy in bin n.

It is through relation (A6) that the fluxes derived for individual energy bins depend on the chosen spectral shape, and thus on the data in all energy bins and time periods used in the determination of χ^2. However, it is the case for GRIP that the fluxes derived in this fashion are relatively insensitive to changes in the input spectrum, and these systematic errors are small compared to the statistical errors. For the case of 1E 1740.7−2942, varying the spectral index between 0 and 4 resulted in changes in the derived fluxes of less than 12%.

In order to search for time variability, the average in equation (A5) is taken over energy bins rather than time periods. This method provides a measurement of the flux normalization for each time period. The product of this normalization and the spectral shape (cf. eq. [A6]) is then integrated over energy to determine integral fluxes.

REFERENCES

Althouse, W. E., Cook, W. R., Cummings, A. C., Finger, M. H., Prince, T. A., Schindler, S. M., Starr, C. H., & Stone, E. C. 1985, Proc. 19th Internat. Cosmic Ray Conf. (La Jolla), 3, 299

Avni, Y. 1976, ApJ, 210, 642

Bally, J., & Leventhal, M. 1991, Nature, 353, 234

Bazzano, A., La Padula, C., Ubertini, P., & Sood, R. K. 1992, ApJ, 385, L17

Bouchet, L., et al. 1991, ApJ, 383, L45

Chapuis, C. G. L., et al. 1991, in Proc. AIP Conf. 232, Gamma-Ray Line Astrophysics (Paris-Saclay), ed. P. Durouchoux & N. Prantzos (New York: AIP), 52

Cook, W. R., Grunsfeld, J. M., Heindl, W. A., Palmer, D. M., Prince, T. A., Schindler, S. M., Starr, C. H., & Stone, E. C. 1991a, Adv. Space Res. 11, No. 8, 191

Cook, W. R., Grunsfeld, J. M., Heindl, W. A., Palmer, D. M., Prince, T. A., Schindler, S. M., & Stone, E. C. 1991b, ApJ, 372, L75

Cook, W. R., Heindl, W. A., Palmer, D. M., Prince, T. A., Schindler, S. M., Starr, C. H., & Stone, E. C. 1990, Proc. 21st Internat. Cosmic Ray Conf. (Adelaide), 1, 216

Cook, W. R., Palmer, D. M., Prince, T. A., Schindler, S. M., Starr, C. H., & Stone, E. C. 1989, in IAU Symp. 136, The Center of the Galaxy, ed. M. Morris (Dordrecht: Reidel), 581

Cordier, B., Roques, J. P., Churazov, E., & Gilfanov, M. 1991, IAU Circ., No. 5377

Covault, C. E., Manandhar, R. P., & Grindlay, J. E. 1990, Proc. 22d Internat. Cosmic Ray Conf. (Dublin), 1, 21

Fenimore, E. E., Klebesadel, R. W., & Laros, J. G. 1983, in Adv. Space Res. 3, 207

Gehrels, N. 1991, in Proc. AIP Conf. 232 (Paris-Saclay), Gamma-Ray Line Astrophysics, ed. P. Durouchoux & N. Prantzos (New York: AIP), 3

Gehrels, N., Barthelmy, S. D., Teegarden, B. J., Tueller, J., Leventhal, M., & MacCallum, C. J. 1991, ApJ, 375, L13

Gilfanov, M., Churazov, E., Claret, A., & Dezalay, J. P. 1992, IAU Circ., No. 5474

Grunsfeld, J., Cook, W., Heindl, W., Palmer, D., Prince, T., & Schindler, S. 1991, in Proc. 28th Yamada Conf., Frontiers of X-Ray Astronomy (Nagoya), ed. Y. Tanaka & K. Koyama (Tokyo: Universal Academy), 417

Hertz, P., & Grindlay, J. E. 1984, ApJ, 278, 137

Kawai, N., Fenimore, E. E., Middleditch, J., Cruddace, R. G., Fritz, G. G., Snyder, W. A., & Ulmer, M. P. 1988, ApJ, 330, 130

Lampton, M., Margon, B., & Bowyer, S. 1976, ApJ, 208, 177

Levine, A. M., et al. 1984, ApJS, 54, 581

Liang, E. P., & Dermer, C. D. 1988, ApJ, 325, L39

Ling, J. C., Mahoney, W. A., Wheaton, Wm. A., & Jacobson, A. S. 1987, ApJ, 321, L117

Lingenfelter, R. E., & Ramaty, R. 1989, ApJ, 343, 686

Mirabel, I. F., Morris, M., Wink, J., Paul, J., & Cordier, B. 1991, A&A, 251, L43

Mirabel, I. F., Rodriguez, L. F., Cordier B., Paul, J., & Lebrun, F. 1992, Nature, 358, 215

Paul, J., et al. 1990, in Proc. AIP Conf. 232 (Paris-Saclay), Gamma-Ray Line Astrophysics, ed. P. Durouchoux & N. Prantzos (New York: AIP), 17

Prince, T., Grunsfeld, J., Gorham, P., Neugebauer, G., Johnson, N., & Skinner, G. 1991a, BAAS, 23, 1392

Prince, T., Kulkarni, S. R., & Skinner, G. K. 1991b, IAU Circ., No. 5252

Riegler, G. R., Ling, J. C., Mahoney, W. A., Wheaton, Wm. A., & Jacobson, A. S. 1985, ApJ, 294, L13

Riegler, G. R., Ling, J. C., Mahoney, W. A., Wheaton, Wm. A., Willett, J. B., & Jacobson, A. S. 1981, ApJ, 248, L13

Schmitz-Fraysse, M. C., Cordier, B., Gilfanov, M., & Churazov, E. 1992, IAU Circ., No. 5472

Skinner, G. K., et al. 1991, A&A, 252, 172

———. 1987, Nature, 330, 544

Skinner, G. K., Willmore, A. P., Foster, A. J., & Eyles, C. J. 1989, in Proc. Gamma-Ray Observatory Science Workshop, ed. W. N. Johnson (Greenbelt: NASA/Goddard Space Flight Center), 4-191

Sunyaev, R., et al. 1990, in Proc. AIP Conf. 232, Gamma-Ray Line Astrophysics (Paris-Saclay), ed. P. Durouchoux & N. Prantzos (New York: AIP), 29

———. 1991, ApJ, 383, L49

Sunyaev, R. A., & Titarchuk, L. G. 1980, A&A, 86, 121